

1 **High-sensitivity lateral flow immunoassay with a fluorescent lanthanide nanoparticle label**

2 Teppo Salminen^{1,*}, Eevi Juntunen¹, Sheikh M. Talha¹, Kim Pettersson¹

3

4 ¹*Department of Biotechnology, University of Turku, Turku, Finland*

5

6

7 ***Running title:*** *Developing a high-sensitivity fluorescent LF assay*

8

9

10

11

12

13

14

15

16

17

18

19

20

21 *Corresponding author: Teppo Salminen

22 Department of Biotechnology, University of Turku, Kiinamylynkatu 10, FI-20520 Turku, Finland.

23 Tel: +358-50-5726386, E-mail: tjsalm@utu.fi

24 **Abstract**

25 Lateral flow (LF) immunoassays are commonly used for point-of-care testing and typically incorporate
26 visually read reporters, such as gold particles. To improve sensitivity and develop quantitative LF
27 immunoassays, visual reporters can be replaced by fluorescent reporters detected by an instrument.
28 In this study, we used fluorescent europium(III) chelate doped nanoparticle (Eu-np) reporters to
29 develop a quantitative high-sensitivity LF immunoassay for free prostate specific antigen (fPSA).
30 Furthermore, we tested different simplified formats of the assay and the effect of different modifiable
31 parameters on the detection limit of the assay: dynamic range, assay duration and number of assay
32 steps. The molar detection limits of the different assay formats were compared with published
33 detection limits of LF immunoassays with different reporters. The cutoff was calculated from 11
34 female serum samples. The detection limit of the sensitivity optimized fPSA assay with fPSA spiked
35 into pooled female serum was 0.01 ng/ml, which is approximately 100-fold lower than the most
36 sensitive gold particle LF assays and 10-fold lower than other Eu-np and carbon nanoparticle based LF
37 immunoassays. Thus, Eu-np reporters can be used to develop highly sensitive and quantitative LF
38 immunoassays.

39 **Keywords:** Prostate specific antigen, lateral flow, fluorescent, immunoassay

40 **1. Introduction**

41 Lateral flow (LF) immunoassays have long been considered ideal for point-of-care testing of diseases
42 and environmental samples due to their simplicity and ease of use. Typically, LF immunoassays use
43 visually read reporters, such as blue latex beads, carbon black nanoparticles, silver enhanced gold and,
44 most importantly, colloidal gold nanoparticles [1]. To improve the sensitivity of the LF assays, magnetic
45 and fluorescent reporters have also been incorporated into LF assays as reporters. These reporters
46 require an instrument for detection, which increases the price and complexity of the test. On the other
47 hand, an instrument-based read-out also provides the advantages of quantification and objective
48 interpretation of the results. Additionally, the instrument can archive and transmit the results
49 automatically. These advantages decrease the risk of operator mistakes and thus many LF assays with
50 traditional visually read reporters have also incorporated automated readers.

51 However, despite these recent reporter improvements the current LF immunoassays still lack the
52 sufficiently precise quantitation and high sensitivity needed to meet the performance of central
53 laboratory assays. Additionally, these goals of quantitation and sensitivity should be met with a
54 sufficiently simple assay protocol in order to retain the simplicity advantage of LF immunoassays.
55 Previously, we have shown that the LF immunoassay sensitivity and signal-to-noise ratio can be

56 improved significantly with fluorescent europium(III) chelate doped nanoparticles (Eu-np) as reporters
57 [2]. Some demonstrations of LF immunoassays for different biomarkers using Eu-np reporters have
58 also been published [3-7]. Also, Eu-np can provide a 100-fold improvement in sensitivity when
59 comparing Eu-np and colloidal gold nanoparticles in the same LF test with identical binders [5,8]. In
60 addition to Eu-np, quantum dot fluorescent nanoparticles have provided sensitivity improvements in
61 LF when compared to colloidal gold [9][10]. Even colloidal gold nanoparticle label sensitivity can be
62 improved, by improving the visual intensity of the signal with gold-nanoparticle-decorated silica
63 nanorods or dual gold label assays [11] [12].

64 In this study, we explore the critical parameters of a LF immunoassay, which affect the dynamic range,
65 assay duration, number of assay steps and sensitivity of the final test. Significant improvements in
66 these aspects of the assay are possible by substituting the normal visual reporters with fluorescent
67 reporters. The LF assay format also has inherent limitations that can be charted through systematic
68 testing of different parameters of the assay. In order to demonstrate the potential of Eu-np reporters
69 and chart the limitations of simple yet sensitive LF assays with a real immunoassay, we developed a
70 highly sensitive yet simple and rapid LF assay for free prostate specific antigen (fPSA).

71 Prostate-specific antigen (PSA) is a human kallikrein protease produced in prostatic epithelial cells
72 [13]. The level of PSA in blood is an important marker for early detection of prostate cancer and also
73 for the recurrence of the cancer after treatment [14]. Current central laboratory PSA immunoassays
74 have limits of detection between 0.008 ng/ml and 0.07 ng/ml [15]. PSA in the bloodstream occurs in
75 complexed (65 – 95 % of total PSA) and free (5 – 35 %) forms [16]. The ratio of fPSA to total PSA in
76 blood can be used to aid the distinguishing of prostate cancer from benign prostatic hyperplasia [17].
77 For example, if the total PSA level is between 4 and 10 ng/ml, a cut-off of <25 % fPSA can be used to
78 select patients for biopsy [18]. Therefore, a specific fPSA measurement is a useful addition to diagnosis
79 of prostate cancer, along with other PSA based serum markers [19]. However, in this study the fPSA
80 assay functions also as a model analyte for exploring the improvements to LF immunoassays gained
81 by using fluorescent reporters.

82 **2. Materials and Methods**

83 *2.1 Preparation of assay materials*

84 Polyclonal mouse IgG (Biodesign, Saco, ME, USA) and H117 mouse monoclonal anti-PSA antibody
85 (University of Turku) were covalently coupled with biotin isothiocyanate (BITC) to form biotinylated
86 conjugates. The conjugation reaction contained 2 mg/ml of the antibody and a 100-fold excess of BITC
87 in 50 mM carbonate buffer (pH 9.8). The reaction was incubated for 4 h at room temperature and

88 excess BITC was separated from the conjugate by NAP-5 and NAP-10 columns (Amersham Pharmacia
89 Biotech, Uppsala, Sweden), with the biotin-antibody conjugates eluted to 10 mM Tris-HCl buffer (pH
90 8.0).

91 Carboxyl-modified Eu(III)-chelate-doped OptiLink polystyrene nanoparticles with a diameter of
92 107 nm (Seradyn, Indianapolis, IN, USA) were covalently linked with anti-PSA antibody 5A10, which
93 binds to an epitope specific for free PSA [20], and with both biotinylated and non-biotinylated
94 polyclonal mouse-IgG (Biosdesign, Saco, ME, USA), as described previously [21]. The resulting anti-PSA-
95 Eu nanoparticles and bio-mIgG-Eu nanoparticles were used as reporters in the LF assays. The
96 recombinant PSA used as standard was produced and purified as described by Rajakoski et. al. [22].

97 The test and control lines on the LF strips were printed with a Linomat 5 non-contact printer (CAMAG,
98 Muttenz, Switzerland) onto a Hi-Flow Plus HF180 or HF90 nitrocellulose membrane (Millipore,
99 Bedford, MA, USA). The streptavidin (SA) test lines were printed in 10 mM citrate-phosphate buffer
100 (pH 5.0). The biotinylated PSA capture antibody H117 was printed in 10 mM Tris-HCl buffer (pH 8.0),
101 with an optimized final density of 0.25 $\mu\text{g}/\text{cm}$ (result not shown). The control line of 0.4 $\mu\text{g}/\text{cm}$ of
102 rabbit—anti-mouse polyclonal antibody was printed at a distance of 6 mm from the test line in 10 mM
103 Tris-HCl buffer (pH 8.0). Before printing the lines, the nitrocellulose membrane was attached to an
104 adhesive backing plastic (G&L Precision Die Cutting, San Jose, CA, USA). After printing, the membranes
105 were dried in +35°C for 2 h. Subsequently, a cellulose absorption pad (Millipore) and a glass fiber feed
106 pad were attached overlapping the nitrocellulose. This assembled membrane card was then cut into
107 5 mm wide lateral flow strips.

108 The reaction buffer used for reagent dilutions and wash steps consisted of 10 mM phosphate buffer
109 (pH 7.4), 135 mM NaCl, 0.5 % Polysorbate 20, 1 % BSA (Bioreba, Reinach, Germany). The female serum
110 samples used for measurement of blank signal were from informed healthy volunteer donors.

111 *2.2 Streptavidin test line optimization*

112 Different densities of SA ranging from 0.5 to 128 $\mu\text{g}/\text{cm}$ were printed and dried on the LF strips. The
113 density of SA was calculated in micrograms per centimeter of test line, each strip containing a 5 mm
114 test line. Optimal SA density was tested by performing an assay with bio-mIgG and mIgG coated Eu-
115 nanoparticles on the SA LF strips not containing the biotinylated capture antibody. Firstly, 10^7 bio-
116 mIgG or mIgG coated Eu-nanoparticle reporters per strip were added to the SA LF strips in 20 μl of
117 reaction buffer, together with 18 nmol of d-biotin per strip. Adding this high concentration of d-biotin
118 to block a constant portion of the binding sites was necessary to ensure that the bio-mIgG
119 nanoparticles were not the limiting reagent in the assay. This is because the SA line contains a much

120 higher number of biotin binding sites than the total number of biotin molecules on the bio-mIgG
121 nanoparticles. Using only bio-mIgG nanoparticles would have resulted in a constant signal from lines
122 with different concentrations of SA, since the usable concentrations of bio-mIgG nanoparticles are too
123 low to saturate the SA line.

124 Secondly, after reporter absorption the strips were washed by adding 80 μ l of reaction buffer. After
125 reaction buffer absorption, the strips were dried in room temperature and the long-lifetime Eu(III)-
126 chelate fluorescence was measured with a Victor X4 multilabel reader (Perkin-Elmer/Wallac, Turku,
127 Finland) in a time-resolved europium measurement.

128 *2.3 LF fPSA assay procedure*

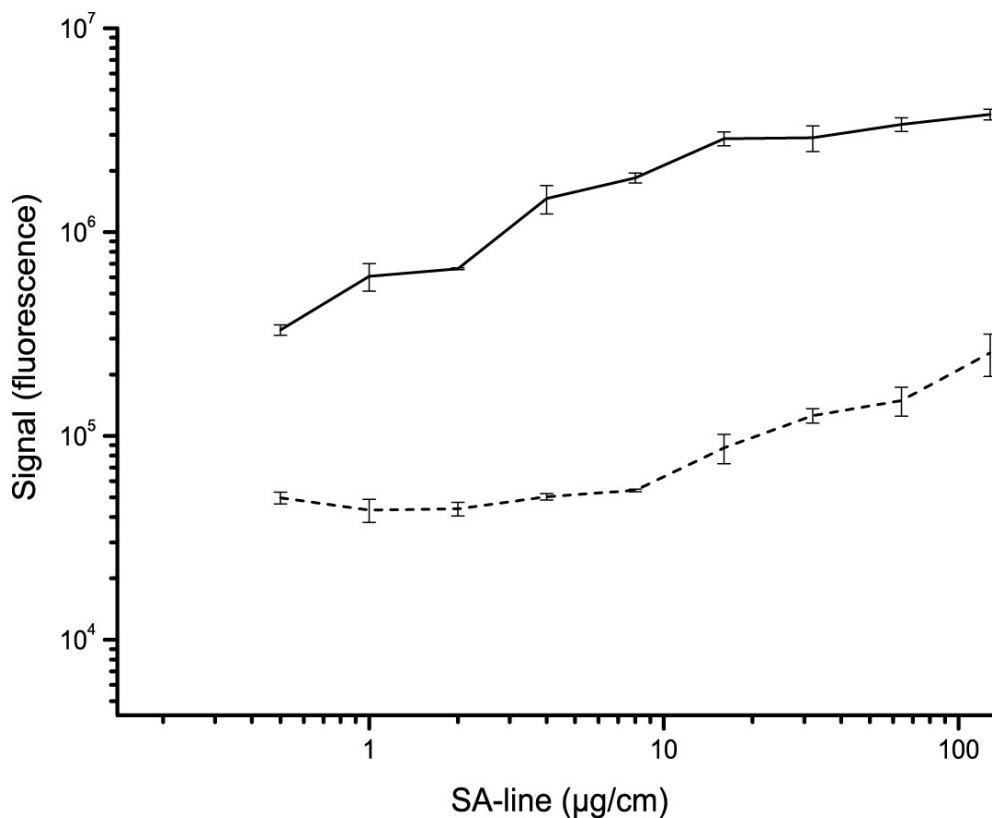
129 In the standard LF fPSA assay procedure, 10 μ l of PSA spiked pooled female serum sample and 20 μ l
130 of reaction buffer containing 10^8 particles of anti-PSA-Eu were added to each strip. Immediately after
131 adding the anti-PSA-Eu, the strip was washed by adding 20 μ l of reaction buffer and left to run in room
132 temperature for 25 minutes before measurement. In the signal development assay, the strips were
133 measured sequentially approximately every 70 seconds after adding the sample and reporter. The
134 measurement was repeated during the liquid flow through the membrane for a total of 27 minutes.
135 All assays had spiked pooled female serum as the sample matrix.

136

137 **3. Results**

138 *3.1 Density of streptavidin test line*

139 The optimal streptavidin density on the test line was tested by comparing the capacity of different
140 density lines to bind bio-mIgG-Eu nanoparticles with the unspecific binding of mIgG-Eu nanoparticles.
141 The bio-mIgG-Eu nanoparticles show the actual relevant binding capacity for nanoparticle reporters;
142 the actual biotin binding capacities of the various densities of SA line may be higher, but steric
143 hindrances caused by the large sized nanoparticles should lower the effective binding capacity. The
144 nanoparticle binding capacity of the SA line increases up to a density of 8 – 16 μ g/cm of SA (Fig. 1).
145 Taking the mIgG-Eu nanoparticle background into account, the maximal signal-to-background ratio is
146 achieved between 4 and 16 μ g/cm of SA. LF strips with 4 μ g/cm of SA were used in the fPSA assays.



147

148 **Fig. 1** The binding capacity and background of streptavidin test lines with different concentrations of
 149 streptavidin. Solid line shows the nanoparticle binding capacity of streptavidin lines with different
 150 concentrations of streptavidin, tested by adding biotinylated mouse-IgG coated Eu(III)-nanoparticles
 151 on the strip. Dashed line shows the unspecific nanoparticle binding on streptavidin lines, tested with
 152 non-biotinylated but otherwise identical mouse-IgG coated Eu(III)-nanoparticles. Standard deviations
 153 of three replicates are depicted as error bars. The streptavidin concentration chosen to be used in
 154 subsequent assays was 4 µg/cm

155

156 3.2 Detection limits of different types of assays

157 The limit of detection (LoD) was calculated from the standard curve, with the cutoff calculated by the
 158 following equation:

159

$$LoD = \mu_B + 1.645\sigma_B + 1.645\sigma_S$$

160

161 Where μ_B is the mean of blank measurements, σ_B is standard deviation of blank measurements and σ_S
 162 is the standard deviation of low sample concentration measurements. The blank signal was the
 163 average signal of 11 measured female sera with a total of 99 replicates. The LoD was tested for the

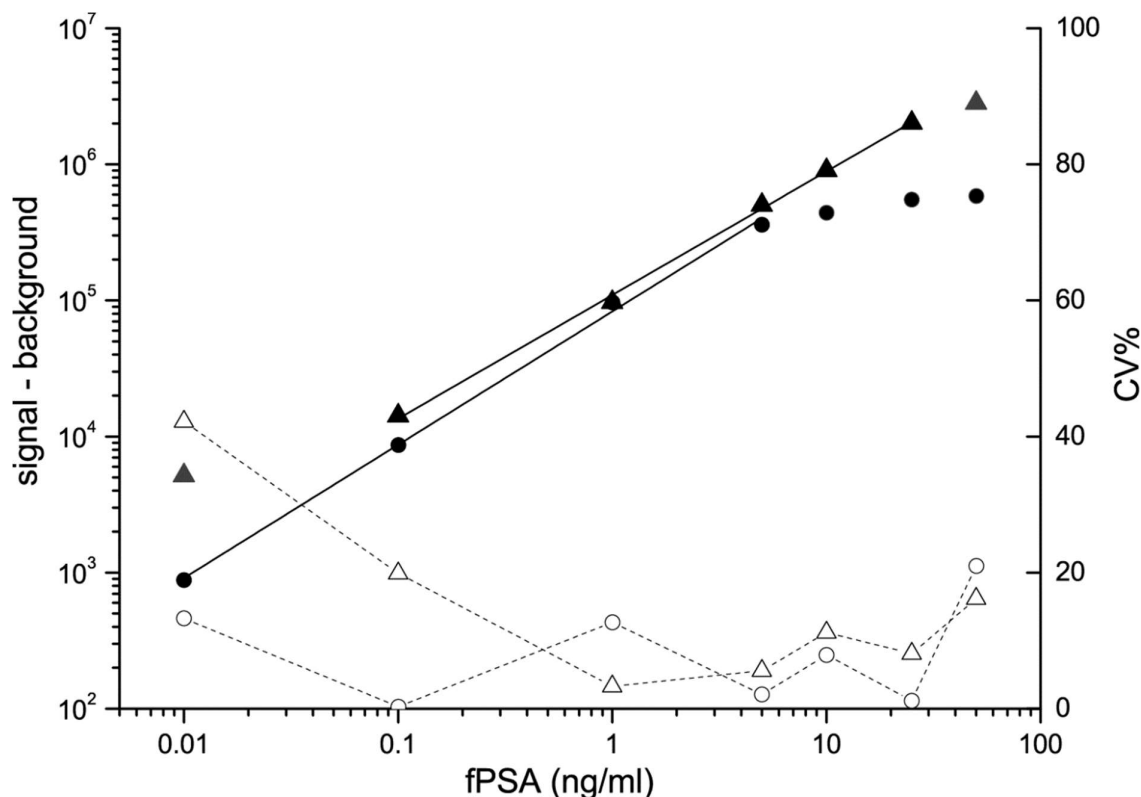
164 sensitivity optimized fPSA LF assay and three variations of the assay protocol (Table 1). The assay
 165 optimized for high sensitivity had a LoD of 0.01 ng/ml.

166 **Table 1.** The limits of detection of the different variations of fPSA LF assays. Sensitivity optimized assay is the
 167 baseline for the other variations and 10^9 particles/strip is tested in order to shift the dynamic range. Using a fast
 168 HF75 nitrocellulose shortens the assay time and removing the wash simplifies the assay. The limit of detection
 169 is shown for each variation in ng/ml and mol/L. The assay modifications reduce the turnaround time and the
 170 number of steps needed to complete the assay but result in increased limits of detection.

Assay protocol:	Limit of detection (ng/ml):	Molarity at detection limit (M)	turnaround time (min)	number of assay steps
Sensitivity optimized assay	0.010	3.5×10^{-13}	21	2
10^9 particles/strip	0.063	22×10^{-13}	21	2
Fast HF75 nitrocellulose	0.014	5.1×10^{-13}	17	2
No wash	0.058	20×10^{-13}	21	1

171

172 To test the possibility of shifting the dynamic range of the assay to higher concentrations, reporter Eu-
 173 np amount was increased ten-fold to 10^9 particles/strip. Compared to the assay with 10^8
 174 particles/strip, the upper limit of linearity increased from 5 to 25 ng/ml of PSA (R-square 0.998 for
 175 both Eu-np amounts) (Fig. 2). The LoD with the higher nanoparticle amount was 0.063 ng/ml.

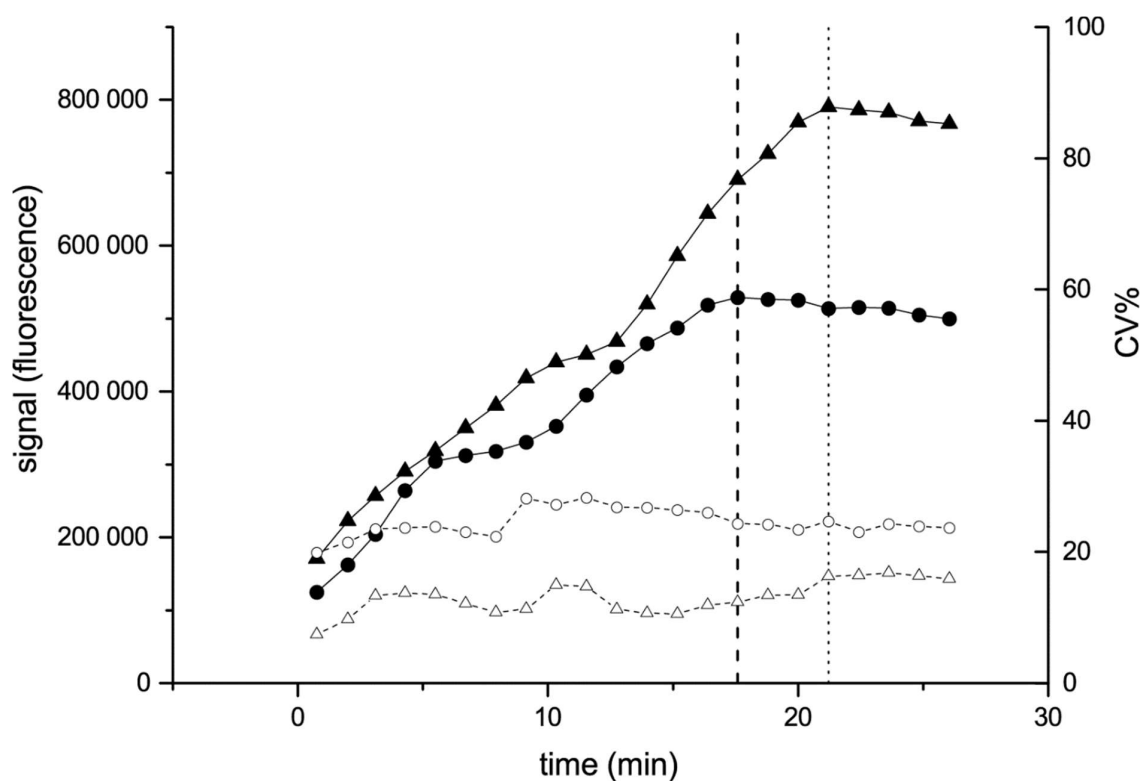


176

177 **Fig. 2** fPSA LF assay dynamic range with 10^8 particles/strip (●) and 10^9 particles/strip (▲) of the anti-
 178 PSA-Eu nanoparticle reporter. With 10^8 and 10^9 nanoparticles per strip, the assay is linear up to 5
 179 ng/ml and 25 ng/ml of fPSA, respectively. Coefficients of variation (%) with three replicates are shown
 180 with dashed lines and empty symbols

181

182 In order to decrease the time the assay takes to reach the maximum signal level, the flow speed of the
 183 sample and reporter conjugate was increased by using a larger pore size nitrocellulose membrane.
 184 The assay with the faster flow speed HF75 nitrocellulose reached maximum signal after 17 minutes,
 185 compared to the 21 minutes of the normal assay with HF180 nitrocellulose (Fig. 3). The LoD with HF75
 186 nitrocellulose was 0.014 ng/ml.

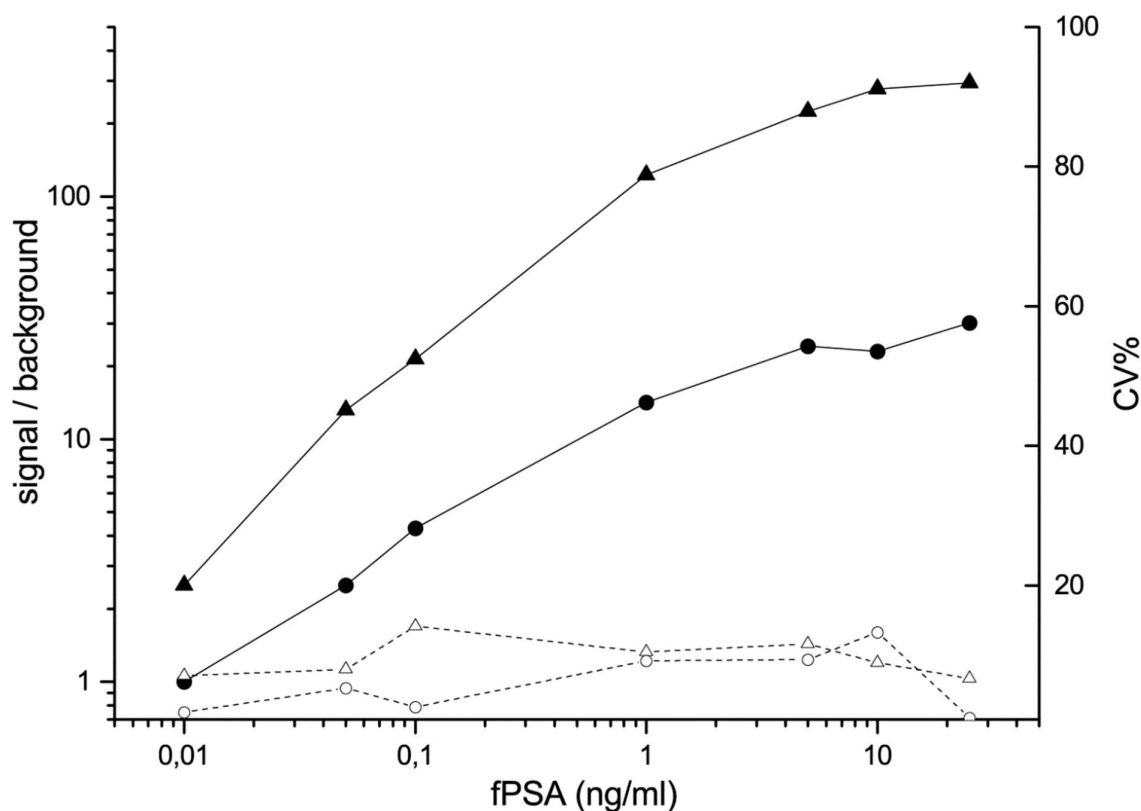


187

188 **Fig. 3** Signal development after adding the sample to the strip in the fPSA assay with HF75 (●) and
 189 HF180 (▲) nitrocellulose membranes used in the assays. The assay reached maximum signal after 17
 190 minutes (dashed line) with HF75 nitrocellulose and after 21 min (dotted line) with HF180
 191 nitrocellulose. Coefficients of variation (%) with three replicates are shown with dashed lines and
 192 empty symbols

193

194 The standard assay protocol included a wash step comprising 20 μ l/strip of reaction buffer. When the
 195 assay was simplified by eliminating this wash step, the LoD was 0.058 ng/ml (Fig. 4).



196

197 **Fig. 4** fPSA LF assay signal/background ratio with a wash step (▲) and without a wash step (●). The
 198 LoD with and without a wash step is 0.01 ng/ml and 0.058 ng/ml, respectively. Coefficients of
 199 variation (%) with three replicates are shown with dashed lines and empty symbols

200

201 4. Discussion

202 In this study, we have developed a highly sensitive LF assay for fPSA with fluorescent Eu-nanoparticles
 203 as reporters. The most sensitive variation of the assay protocol had a limit of detection of 0.010 ng/ml
 204 (3.5×10^{-13} M). We also tested the assay with different simpler assay protocol variations to test the
 205 effect of these parameters on the sensitivity of the assay. The LoD in these protocols varied from 0.014
 206 to 0.058 ng/ml (5.1×10^{-13} - 20×10^{-13} M) (Table 1). The simplification of the assay protocols consisted
 207 of removing the wash step to achieve a one-step protocol and using a fast nitrocellulose to decrease
 208 the time the assay takes to reach the maximum signal.

209 Most published LF assays for PSA set the cutoff at the clinically relevant 4 ng/ml concentration of total
 210 PSA and thus do not optimize the assay for high analytical sensitivity [23-26]. However, ultrasensitive
 211 PSA assays can help in early detection of prostate cancer recurrence after radical prostatectomy, and
 212 some very sensitive PSA assays have been developed [27]. Li et al. developed a quantitative LF assay
 213 for PSA with quantum dot nanobead-labels, achieving a sensitivity of 0.33 ng/ml (1×10^{-11} M) [28].

214 Additionally, some published microtiter well-based immunoassays for PSA using different reporter
215 technologies have reported very low limits of detection. Particularly, Soukka et al used Eu-np reporters
216 similar to the particles used in this publication for ultrasensitive detection of fPSA in wells achieving a
217 limit of detection of 1.3×10^{-15} M with 30 μ l of sample [29]. With 5 μ l of sample, the limit of detection
218 was 1.3×10^{-14} M, which is equivalent to 59 zmol of fPSA in the sample. The corresponding lowest
219 detected amount in our fPSA LF assay with 10 μ l sample volume was 3500 zmol. Also, published ELISA
220 and chemiluminescence-reporter assays for fPSA had sensitivities in the same range as the fPSA LF
221 assay, 2.7×10^{-13} M for the ELISA and 2.3×10^{-13} M for the chemiluminescence well assay [30,31].
222 However, the sensitivity of different assays even for the same analyte is not affected only by the assay
223 type or the label, but also the choice of binders. Therefore, direct label comparison between assays is
224 difficult.

225 Taking this limitation into account, the limit of detection of our developed LF immunoassay can also
226 be compared to other LF immunoassays for different protein markers, with the published limits of
227 detection converted to molarity as shown by Gordon and Michel [32]. In their review, the detection
228 limits of LF immunoassays based on gold particle reporters varied from 10^{-5} to 3×10^{-11} M. However,
229 various types of reporters used in LF immunoassays have achieved lower detection limits compared
230 to gold reporters.

231 LF immunoassays using Eu-np reporters for various analytes achieved detection limits down to the 10^{-12}
232 M range [3,5,33,34]. Carbon nanoparticle based assays had similar detection limits of approximately
233 10^{-12} M [35-37]. Experimental LF assays for bacterial toxins using dye-containing liposomes with toxin
234 receptors incorporated in the lipid bilayer as reporters reached detection limits of 10^{-12} and 10^{-16} M
235 [38,39]. Finally, LF immunoassays with up-converting phosphor reporters had detection limits ranging
236 from 10^{-12} to 10^{-15} M [40-43].

237 However, there are naturally a number of limitations to an approach where different LF immunoassay
238 reporters are compared across a variety of protein markers and publications. First, each protein
239 marker has different binder antibodies with different affinities. Secondly, the assay protocols,
240 materials and time to results vary among assays. Thirdly, assays for different proteins have been tested
241 in different sample matrices, some of which may be more challenging for the assays than others.
242 Finally, even the methods used to determine the detection limit vary among the published assays.
243 Nevertheless, a broad comparison between different reporter types can be made. When compared to
244 the other published LF immunoassays, the lowest detection limit of 3.5×10^{-13} M achieved with our
245 published fPSA LF immunoassay is approximately 100-fold lower than the most sensitive gold particle

246 LF assays and 10-fold lower than other Eu-np and carbon nanoparticle based LF assays. A similar or
247 even superior detection limit can be reached with up-converting phosphor reporters.

248 Like all fluorescent reporters, Eu-nanoparticles require an instrument for detection. In addition to the
249 sensitivity enhancement of instrument-based reading, use of an instrument also enables quantitative
250 assays and lowers the possibility of human error in result reading and data management [44]. Because
251 of these advantages, even LF assays with visually readable gold particle reporters are often read by an
252 optical instrument. Due to the conflicting needs of sensitive instrumentation and portability as well as
253 affordability, the practical success of fluorescence based LF immunoassays is largely dependent on the
254 availability of low-cost miniaturized detection instruments. This need for portable LF readers capable
255 of detecting Eu-nanoparticle labels is already being met. For example, an LF immunoassay for influenza
256 using Eu-np reporters together with a dedicated reader is in the market [45,46]. Also, published LF
257 immunoassays with Eu-np reporters have used commercially available portable readers [7,34,47] or
258 even a digital camera together with an ultraviolet light source [2,5,48] as a detection instrument.
259 Uniquely, Preechadakasedkit et al developed reporter particles with a gold core coated with europium
260 chelate-doped silica coating, allowing both visual and instrument-based fluorescent detection in a LF
261 assay [49].

262 In rapid point-of-care assays, the critical parameters that affect the limit of detection force a
263 compromise between sensitivity on one hand and speed and simplicity on the other. Particularly the
264 elimination of a separate wash step simplifies the assay but also increases the limit of detection from
265 0.01 ng/ml to 0.058 ng/ml. Additionally, the adjustment of the dynamic range for samples with higher
266 concentrations of the analyte may affect the sensitivity of the assay. In the case of our LF
267 immunoassay, the dynamic range is approximately three orders of magnitude. This forces a
268 compromise in the detection limit in a quantitative assay depending on the desired quantitative range.
269 A tenfold increase in the number of reporter particles increases upper limit of linearity approximately
270 five-fold, with a similar increase in the detection limit (Fig. 2).

271 The time for the sensitivity optimized assay to reach the stable maximum signal is 21 minutes (Fig. 3).
272 This time can be shortened by using a nitrocellulose membrane with a larger average pore size and
273 thus faster flow rate. The effect of using larger pore size nitrocellulose is modest; use of HF75
274 nitrocellulose, which has a 2.4-fold faster flow rate compared with HF180, only decreases the assay
275 time by 4 minutes, from 21 minutes to 17 minutes, while increasing the detection limit from 0.010
276 ng/ml to 0.014 ng/ml. In order to shorten the assay time, the assay can also be measured before the
277 maximum signal is reached. However in this case, in addition to a compromise in sensitivity, the

278 calibration curve for a quantitative assay has to be adjusted to the exact measurement time point due
279 to constant change in the signal level caused by ongoing flow in the membrane.

280 In conclusion, it is possible to develop a highly sensitive quantitative lateral flow assay for fPSA by
281 using fluorescent reporters. In order to achieve a simple and fast assay, a compromise has to be made
282 between ease of use and sensitivity. Nevertheless, even in the simplest format, the developed assay
283 is quantitative and the very sensitive compared to a LF assay based on standard gold particle reporters.

284 **Declarations of interest:** none

285 This research did not receive any specific grant from funding agencies in the public, commercial, or
286 not-for-profit sectors.

287

288 **References:**

- 289 1. Linares EM, Kubota LT, Michaelis J, Thalhammer S (2012) Enhancement of the detection limit for
290 lateral flow immunoassays: evaluation and comparison of bioconjugates. *Journal of*
291 *immunological methods* 375: 264-270. doi:10.1016/j.jim.2011.11.003 [doi]
- 292 2. Juntunen E, Myyrylainen T, Salminen T, Soukka T, Petterson K (2012) Performance of fluorescent
293 europium(III) nanoparticles and colloidal gold reporters in lateral flow bioaffinity assay. *Anal*
294 *Biochem* 428: 31-38. doi:10.1016/j.ab.2012.06.005
- 295 3. Rundstrom G, Jonsson A, Martensson O, Mendel-Hartvig I, Venge P (2007) Lateral flow
296 immunoassay using Europium (III) chelate microparticles and time-resolved fluorescence for
297 eosinophils and neutrophils in whole blood. *Clinical chemistry* 53: 342-348.
298 doi:clinchem.2006.074021 [pii]
- 299 4. Nabatiyan A, Baumann MA, Parpia Z, Kelso D (2010) A lateral flow-based ultra-sensitive p24 HIV
300 assay utilizing fluorescent microparticles. *Journal of acquired immune deficiency syndromes*
301 (1999) 53: 55-61. doi:10.1097/QAI.0b013e3181c4b9d5 [doi]
- 302 5. Xia X, Xu Y, Zhao X, Li Q (2009) Lateral Flow Immunoassay Using Europium Chelate-Loaded Silica
303 Nanoparticles as Labels. *Clinical Chemistry* 55: 179-182. doi:10.1373/clinchem.2008.114561
- 304 6. Salminen T, Knuutila A, Barkoff AM, Mertsola J, He Q (2018) A rapid lateral flow immunoassay for
305 serological diagnosis of pertussis. *Vaccine* 36: 1429-1434. doi:10.1016/j.vaccine.2018.01.064
- 306 7. Song C, Zhi A, Liu Q, Yang J, Jia G, et al. (2013) Rapid and sensitive detection of β -agonists using a
307 portable fluorescence biosensor based on fluorescent nanosilica and a lateral flow test strip.
308 *Biosensors and Bioelectronics* 50: 62-65. doi:https://doi.org/10.1016/j.bios.2013.06.022
- 309 8. Zhang F, Zou M, Chen Y, Li J, Wang Y, et al. (2014) Lanthanide-labeled immunochromatographic
310 strips for the rapid detection of *Pantoea stewartii* subsp. *stewartii*. *Biosensors &*
311 *bioelectronics* 51: 29-35. doi:10.1016/j.bios.2013.06.065 [doi]
- 312 9. Di Nardo F, Anfossi L, Giovannoli C, Passini C, Gofman VV, et al. (2016) A fluorescent
313 immunochromatographic strip test using Quantum Dots for fumonisins detection. *Talanta*
314 150: 463-468. doi:https://doi.org/10.1016/j.talanta.2015.12.072
- 315 10. Foubert A, Beloglazova NV, De Saeger S (2017) Comparative study of colloidal gold and quantum
316 dots as labels for multiplex screening tests for multi-mycotoxin detection. *Analytica Chimica*
317 *Acta* 955: 48-57. doi:https://doi.org/10.1016/j.aca.2016.11.042
- 318 11. Xu H, Chen J, Birrenkott J, Zhao JX, Takalkar S, et al. (2014) Gold-Nanoparticle-Decorated Silica
319 Nanorods for Sensitive Visual Detection of Proteins. *Analytical Chemistry* 86: 7351-7359.
320 doi:10.1021/ac502249f

- 321 12. Choi DH, Lee SK, Oh YK, Bae BW, Lee SD, et al. (2010) A dual gold nanoparticle conjugate-based
322 lateral flow assay (LFA) method for the analysis of troponin I. *Biosens Bioelectron* 25: 1999-
323 2002. doi:10.1016/j.bios.2010.01.019
- 324 13. Yousef GM, Diamandis EP (2002) Expanded human tissue kallikrein family--a novel panel of
325 cancer biomarkers. *Tumour Biol* 23: 185-192. doi:10.1159/000064027
- 326 14. Heidenreich A, Aus G, Bolla M, Joniau S, Matveev VB, et al. (2008) EAU guidelines on prostate
327 cancer. *European urology* 53: 68-80. doi:S0302-2838(07)01145-1 [pii]
- 328 15. Sharma S, Zapatero-Rodríguez J, O'Kennedy R (2017) Prostate cancer diagnostics: Clinical
329 challenges and the ongoing need for disruptive and effective diagnostic tools. *Biotechnology*
330 *Advances* 35: 135-149. doi:<http://doi.org/10.1016/j.biotechadv.2016.11.009>
- 331 16. Lilja H, Christensson A, Dahlen U, Matikainen MT, Nilsson O, et al. (1991) Prostate-specific
332 antigen in serum occurs predominantly in complex with alpha 1-antichymotrypsin. *Clinical*
333 *chemistry* 37: 1618-1625.
- 334 17. Peltola MT, Niemela P, Alanen K, Nurmi M, Lilja H, et al. (2011) Immunoassay for the
335 discrimination of free prostate-specific antigen (fPSA) forms with internal cleavages at
336 Lys((1)(4)(5)) or Lys((1)(4)(6)) from fPSA without internal cleavages at Lys((1)(4)(5)) or
337 Lys((1)(4)(6)). *Journal of immunological methods* 369: 74-80. doi:10.1016/j.jim.2011.04.006
338 [doi]
- 339 18. Catalona WJ, Hudson MA, Scardino PT, Richie JP, Ahmann FR, et al. (1994) Selection of optimal
340 prostate specific antigen cutoffs for early detection of prostate cancer: Receiver operating
341 characteristic curves. *Journal of Urology* 152: 2037-2042.
- 342 19. Stephan C, Ralla B, Jung K (2014) Prostate-specific antigen and other serum and urine markers in
343 prostate cancer. *Biochimica et Biophysica Acta (BBA) - Reviews on Cancer* 1846: 99-112.
344 doi:<https://doi.org/10.1016/j.bbcan.2014.04.001>
- 345 20. Pettersson K, Piironen T, Seppala M, Liukkonen L, Christensson A, et al. (1995) Free and
346 complexed prostate-specific antigen (PSA): in vitro stability, epitope map, and development
347 of immunofluorometric assays for specific and sensitive detection of free PSA and PSA-alpha
348 1-antichymotrypsin complex. *Clinical chemistry* 41: 1480-1488.
- 349 21. Soukka T, Harma H, Paukkunen J, Lovgren T (2001) Utilization of kinetically enhanced
350 monovalent binding affinity by immunoassays based on multivalent nanoparticle-antibody
351 bioconjugates. *Analytical Chemistry* 73: 2254-2260.
- 352 22. Rajakoski K, Piironen T, Pettersson K, Lovgren J, Karp M (1997) Epitope mapping of human
353 prostate specific antigen and glandular kallikrein expressed in insect cells. *Prostate cancer*
354 *and prostatic diseases* 1: 16-20. doi:10.1038/sj.pcan.4500206 [doi]
- 355 23. Miano R, Mele GO, Germani S, Bove P, Sansalone S, et al. (2005) Evaluation of a new, rapid,
356 qualitative, one-step PSA Test for prostate cancer screening: the PSA RapidScreen test.
357 *Prostate cancer and prostatic diseases* 8: 219-223. doi:4500802 [pii]
- 358 24. Berg W, Linder C, Eschholz G, Schubert J (2001) Pilot study of the practical relevance of a one-
359 step test for prostate-specific antigen in capillary blood to improve the acceptance rate in
360 the early detection program of prostate carcinoma. *International urology and nephrology*
361 32: 381-388.
- 362 25. Dok An C, Yoshiki T, Lee G, Okada Y (2001) Evaluation of a rapid qualitative prostate specific
363 antigen assay, the One Step PSA(TM) test. *Cancer letters* 162: 135-139.
364 doi:S0304383500006157 [pii]
- 365 26. Jung K, Zachow J, Lein M, Brux B, Sinha P, et al. (1999) Rapid detection of elevated prostate-
366 specific antigen levels in blood: performance of various membrane strip tests compared.
367 *Urology* 53: 155-160. doi:S0090-4295(98)00419-1 [pii]
- 368 27. Tilki D, Kim SI, Hu B, Dall'Era MA, Evans CP (2015) Ultrasensitive Prostate Specific Antigen and its
369 Role after Radical Prostatectomy: A Systematic Review. *The Journal of Urology* 193: 1525-
370 1531. doi:<https://doi.org/10.1016/j.juro.2014.10.087>

- 371 28. Li X, Li W, Yang Q, Gong X, Guo W, et al. (2014) Rapid and Quantitative Detection of Prostate
372 Specific Antigen with a Quantum Dot Nanobeads-Based Immunochromatography Test Strip.
373 ACS Applied Materials & Interfaces 6: 6406-6414. doi:10.1021/am5012782
- 374 29. Soukka T, Paukkunen J, Harma H, Lonnberg S, Lindroos H, et al. (2001) Supersensitive time-
375 resolved immunofluorometric assay of free prostate-specific antigen with nanoparticle label
376 technology. *Clinical chemistry* 47: 1269-1278.
- 377 30. Matsumoto K, Konishi N, Hiasa Y, Kimura E, Takahashi Y, et al. (1999) A highly sensitive enzyme-
378 linked immunoassay for serum free prostate specific antigen (f-PSA). *Clinica Chimica Acta*
379 281: 57-69. doi:https://doi.org/10.1016/S0009-8981(98)00208-3
- 380 31. Liu A, Zhao F, Zhao Y, Shangguan L, Liu S (2016) A portable chemiluminescence imaging
381 immunoassay for simultaneous detection of different isoforms of prostate specific antigen in
382 serum. *Biosensors and Bioelectronics* 81: 97-102.
383 doi:https://doi.org/10.1016/j.bios.2016.02.049
- 384 32. Gordon J, Michel G (2008) Analytical sensitivity limits for lateral flow immunoassays. *Clinical*
385 *chemistry* 54: 1250-1251. doi:10.1373/clinchem.2007.102491 [doi]
- 386 33. Song X, Knotts M (2008) Time-resolved luminescent lateral flow assay technology. *Anal Chim*
387 *Acta* 626: 186-192. doi:10.1016/j.aca.2008.08.006
- 388 34. Shao XY, Wang CR, Xie CM, Wang XG, Liang RL, et al. (2017) Rapid and Sensitive Lateral Flow
389 Immunoassay Method for Procalcitonin (PCT) Based on Time-Resolved
390 Immunochromatography. *Sensors (Basel)* 17. doi:10.3390/s17030480
- 391 35. van Dam GJ, Wichers JH, Ferreira TM, Ghatai D, van Amerongen A, et al. (2004) Diagnosis of
392 schistosomiasis by reagent strip test for detection of circulating cathodic antigen. *Journal of*
393 *clinical microbiology* 42: 5458-5461. doi:10.1128/JCM.42.12.5458-61.2004 [pii]
- 394 36. Koets M, Sander I, Bogdanovic J, Doekes G, van Amerongen A (2006) A rapid lateral flow
395 immunoassay for the detection of fungal alpha-amylase at the workplace. *Journal of*
396 *environmental monitoring* : JEM 8: 942-946. doi:10.1039/b605389k [doi]
- 397 37. Parpia ZA, Elghanian R, Nabatiyan A, Hardie DR, Kelso DM (2010) p24 antigen rapid test for
398 diagnosis of acute pediatric HIV infection. *Journal of acquired immune deficiency syndromes*
399 (1999) 55: 413-419. doi:10.1097/QAI.0b013e3181f1afbc [doi]
- 400 38. Ahn-Yoon S, DeCory TR, Durst RA (2004) Ganglioside-liposome immunoassay for the detection of
401 botulinum toxin. *Analytical and bioanalytical chemistry* 378: 68-75. doi:10.1007/s00216-003-
402 2365-4 [doi]
- 403 39. Ahn-Yoon S, DeCory TR, Baeumner AJ, Durst RA (2003) Ganglioside-liposome immunoassay for
404 the ultrasensitive detection of cholera toxin. *Analytical Chemistry* 75: 2256-2261.
- 405 40. Hampl J, Hall M, Mufti NA, Yao YM, MacQueen DB, et al. (2001) Upconverting phosphor
406 reporters in immunochromatographic assays. *Analytical Biochemistry* 288: 176-187.
407 doi:10.1006/abio.2000.4902 [doi]
- 408 41. Corstjens PL, de Dood CJ, van der Ploeg-van Schip JJ, Wiesmeijer KC, Riuttamaki T, et al. (2011)
409 Lateral flow assay for simultaneous detection of cellular- and humoral immune responses.
410 *Clinical biochemistry* 44: 1241-1246. doi:10.1016/j.clinbiochem.2011.06.983 [doi]
- 411 42. Corstjens PL, van Lieshout L, Zuiderwijk M, Kornelis D, Tanke HJ, et al. (2008) Up-converting
412 phosphor technology-based lateral flow assay for detection of Schistosoma circulating
413 anodic antigen in serum. *Journal of clinical microbiology* 46: 171-176. doi:10.1128/JCM.00877-07 [pii]
- 414 43. Juntunen E, Arppe R, Kalliomaki L, Salminen T, Talha SM, et al. (2015) Effects of blood sample
415 anticoagulants on lateral flow assays using luminescent photon-upconverting and Eu(III)
416 nanoparticle reporters. *Analytical Biochemistry* 492: 13-20. doi:10.1016/j.ab.2015.07.013 [pii]
- 417 44. Scherr T, Gupta S, Wright D, Haselton F (2016) Mobile phone imaging and cloud-based analysis
418 for standardized malaria detection and reporting. *Scientific Reports* 7: 1-7. doi:10.1038/s41598-016-08000-4 [pii]
- 419 45. Lee CK, Cho CH, Woo MK, Nyeck AE, Lim CS, et al. (2012) Evaluation of Sofia fluorescent
420 immunoassay analyzer for influenza A/B virus. *Journal of clinical virology : the official*

- 421 publication of the Pan American Society for Clinical Virology 55: 239-243.
422 doi:10.1016/j.jcv.2012.07.008 [doi]
- 423 46. Leonardi GP, Wilson AM, Zuretti AR (2013) Comparison of conventional lateral-flow assays and a
424 new fluorescent immunoassay to detect influenza viruses. *Journal of virological methods*
425 189: 379-382. doi:10.1016/j.jviromet.2013.02.008 [doi]
- 426 47. Liang RL, Deng QT, Chen ZH, Xu XP, Zhou JW, et al. (2017) Europium (III) chelate microparticle-
427 based lateral flow immunoassay strips for rapid and quantitative detection of antibody to
428 hepatitis B core antigen. *Sci Rep* 7: 14093. doi:10.1038/s41598-017-14427-4
- 429 48. Xia X, Xu Y, Ke R, Zhang H, Zou M, et al. (2013) A highly sensitive europium nanoparticle-based
430 lateral flow immunoassay for detection of chloramphenicol residue. *Anal Bioanal Chem* 405:
431 7541-7544. doi:10.1007/s00216-013-7210-9
- 432 49. Preechakasedkit P, Osada K, Katayama Y, Ruecha N, Suzuki K, et al. (2018) Gold nanoparticle
433 core-europium(iii) chelate fluorophore-doped silica shell hybrid nanocomposites for the
434 lateral flow immunoassay of human thyroid stimulating hormone with a dual signal readout.
435 *Analyst* 143: 564-570. doi:10.1039/c7an01799e
- 436
- 437